The hydrogenation of levulinic acid to γ-valerolactone over Cu-ZrO_2 catalysts prepared by a pH-gradient methodology

Igor Orlowski[a], Mark Douthwaite[a], Sarwat Iqbal[a,b], James S. Hayward[a], Thomas E. Davies[a], Jonathan K. Bartley[a], Peter J. Miedziak[a,c], Jun Hirayama[a,d], David J. Morgan[a], David J. Willock[a,*], Graham J. Hutchings[a,*]

* Corresponding authors. Tel: +44 29 2087 4059, Fax: (+44) 2920-874-030; E-mail addresses: hutch@cardiff.ac.uk (G. J. Hutchings), willockdj@cardiff.ac.uk (D. J. Willock).

[a] *Cardiff Catalysis Institute, School of Chemistry, Cardiff University, Main Building, Park Place, Cardiff, CF10 3AT (UK);*

[b] *School of Chemistry, Joseph Bank Laboratories, Beevor St, University of Lincoln, Lincoln, LN6 7DL (UK)*

[c] *School of Applied Sciences, University of South Wales, Pontypridd, CF37 4AT (UK)*

[d] *Institute for Catalysis, Hokkaido University, Sapporo, Hokkaido 001-0021, Japan*

Dedicated to the 70th anniversary of Dalian Institute of Chemical Physics, CAS, China.

Abstract

A novel pH gradient methodology was used to synthesise a series of Cu-ZrO_2 catalysts containing different quantities of Cu and Zr. All of the catalysts were highly selective to the desired product, γ-valerolactone, and are considerably more stable than Cu-ZrO_2 catalysts prepared by other co-precipitation methods for this reaction. Characterisation and further investigation of these catalysts by XRD, BET, SEM and XPS provided insight into the nature of the catalytic active site and the physicochemical properties that lead to catalyst stability. We consider the active site to be the interface between Cu/CuO_x and ZrO_x and that lattice Cu species assist with the dispersion of surface Cu through the promotion of a strong metal support interaction. This enhanced understanding of the active site and roles of lattice and surface Cu will assist with future catalyst design. As such, we conclude that the activity of Cu-ZrO_2 catalysts in this reaction is dictated by the quantity of Cu-Zr interface sites.

Keywords: Cu-ZrO_2; Hydrogenation; Levulinic acid; γ-valerolactone

Biographies

David J. Willock is a Reader in Theoretical and Computational Chemistry at Cardiff University and has been an active researcher in the area of computational chemistry for more than 25 years. He has over 140 publications in the area with a focus on materials chemistry and catalysis. He is a member of the Cardiff Catalysis Institute collaborating closely with experimental research teams on structure and reactivity involving metals, oxides and carbon based materials. His work has covered fundamental studies of surface structure and reactivity in oxidation chemistry and in the hydrogenation of organic molecules with a focus on the development of sustainable catalysis.

Graham Hutchings is Regius Professor of Chemistry at Cardiff University and Director of the Cardiff Catalysis Institute. He studied chemistry at University College London. His early career was with ICI and AECI Ltd where he became interested in gold catalysis. In 1984 he moved to academia and has held chairs at the Universities of Witwatersrand, Liverpool and Cardiff. He was elected a Fellow of the Royal Society in 2009, a Member of Academia Europaea in 2010. He was awarded the Davy Medal of the Royal Society in 2013, the ENI Award for Advanced Environmental Solutions in 2017 and the RSC Faraday Lectureship Prize in 2018.

1. Introduction

Increasing global energy demands and diminishing fossil fuel stores has provided the scientific community with the motivation to develop new and economically viable routes to sustainable energy. As a consequence, there has been a growing interest in biomass valorisation in recent years [1,2]. Lignocellulose is a promising biomass feedstock due to its natural abundance and is often considered to be more viable than first generation biofuel feedstocks, as its production does not compete for arable land with food crops. As such, the development of suitable technology and infrastructure which can efficiently valorise lignocellulosic feedstocks would be hugely beneficial from both a social and economic perspective.

Levulinic acid (LA) has been identified by the US Department of Energy to be one of ten high-value molecules which can be derived from biomass [3]. LA can be produced in high yields from the hydrolysis of hexitols (Scheme 1). This can be done either stoichiometrically using acids [4] or by a catalytic route, over strongly Bronsted acidic materials [5].

While LA does possess some interesting applications as a speciality chemical, far more emphasis has been placed on its numerous routes for valorisation. LA can be converted into a range of useful chemicals including γ-valerolactone (GVL) [6], 1-4 pentanediol and 2-methyltetrahydrofuran (2-MTHF) [7] both of which are considered to be promising fuel additives [8]. Furthermore, GVL can also be used as a monomer for the synthesis of 'green' bio-degradable polymers [9].

GVL possesses many attractive properties which make it a suitable replacement for bio-ethanol; it has a lower vapour pressure, high energy density, high boiling point and does not form an azeotrope with water, making separation far easier [10,11]. In addition, GVL can be further upgraded and used as a feedstock for the production of liquid alkenes (C_8–C_{16} chains) [12]. Currently, the majority of all commercial bio-ethanol is produced by the fermentation of sugars, which are typically sourced from corn or sugar cane. Whilst the process itself is widely accepted as being environmentally friendly, the sustainability of the overall process has been a subject of debate, given that the production of the feedstocks competes for arable land with food crops [13,14]. Technologies to produce ethanol from cellulose do exist, but they are comparatively expensive and therefore, currently only account for a fraction of the global bio-ethanol produced each year [15]. For these reasons, developing an economic and efficient means of producing GVL from LA would be highly advantageous and the hydrogenation of LA over a catalyst is perhaps the most viable method reported to date.

Previous studies have reported the use of both homogeneous and heterogeneous catalysts for the hydrogenation of LA to GVL. Supported ruthenium catalysts perform well for this reaction and consistently deliver excellent GVL yields (> 95%) under relatively mild conditions. As such, Ru-based catalysts are generally accepted as benchmark catalysts for this reaction, and typically comprise of Ru metal loadings between 0.5 – 2 wt% [16–18]. Other noble metals have also been studied, such as

palladium [19,20], gold [21] and platinum [22]. However, due to the relatively high costs associated with noble metals, the application of such elements on an industrial scale is somewhat limiting. As such, there is a drive to develop efficient hydrogenation catalysts comprising of cheap, non-noble metals. Copper has been explored as an alternative to ruthenium for this reaction, and is far more abundant. Rode and co-workers were one of the first to determine that 50 wt% Cu-ZrO_2 and Cu-Al_2O_3 catalysts are active for the hydrogenation of LA and show good selectivity toward GVL [23].

Various bimetallic catalysts containing Cu have also been investigated for the hydrogenation of LA to GVL. Zhang et al.[24] determined that the incorporation of Ag into a Cu/Al_2O_3 catalyst suppressed the leaching of Cu metal during the reaction, which, as a consequence, greatly improved the re-usability of the catalyst. Various studies have also investigated supported Cu-Ni catalysts [25,26]; the presence of Ni improves reaction rates which is attributed to changes in the electronic properties of the Cu. Another study reported that the deposition of Pd onto a Cu-ZrO_2 could result in sequential reaction to produce 1,4-pentanediol and 2-methyl tetrahydrofuran [27]. We too have investigated how the doping of a secondary transition metal onto a Cu-ZrO_2 catalysts affects the performance [28]. Of the metals tested, only Mn provided a promotional effect which was established to be due to an increase in the rate of dissociative H_2 adsorption over the catalyst.

Numerous studies have also investigated the use of sacrificial hydrogen donors such as 2-propanol over supported Cu catalysts [29]. While these approaches are often highly efficient and eliminate the requirement of molecular hydrogen, they are often not as atom efficient as they perhaps appear. In the presence of a supported metal catalysts, the source of hydrogen likely comes from the reformation of the sacrificial alcohol, rather than the via Meerwein-Ponndorf-Verley reduction, which is observed over Sn-β zeolite and amorphous zirconia catalysts [30,31]. It is therefore often the case that greater quantities of the sacrificial alcohol are consumed than substrate.

Despite the abundance of literature in this area, the desirable physicochemical properties of Cu-ZrO_2 catalysts for this reaction remain elusive. The performance of such catalysts have often been attributed to total surface area and/or copper surface area of the catalyst [32,33]. Previously, we synthesised and tested a series of Cu-ZrO_2 catalysts for the hydrogenation of LA to GVL and determined that the active catalysts consisted of large quantities of copper within the ZrO_2 lattice, as well as a surface containing CuO and Cu species [32,33].

Additionally, it was shown that deposition precipitation of copper directly on to the surface of zirconia produced comparatively poorly active catalysts [33]. As such, we believe that the copper sequestered within the bulk is redundant, and that discrete copper on the surface possesses limited catalytic activity, suggesting that it is the interface between copper and zirconia that comprises the active site.

With this in mind, we describe herein a novel catalyst synthesis method aimed at enriching the amount of copper in the surface lattice, reducing the amount of copper locked up within the bulk and present as spectator species on the surface. This should, in turn, reduce the amount of copper required to obtain useful activity, which will further enhance the cost-effectiveness of the material particularly as an alternative to Ru catalysts. We also provide evidence of a strong metal support interaction (SMSI) between Cu and ZrO_2 which is central to the catalytic activity of these catalysts in hydrogenation reactions.

2. Experimental

2.1. Synthesis of $CuZrO_2$ by pH gradient method

For the synthesis of a 50 mol% Cu-ZrO_2 catalyst, the following procedure was followed. $Cu(NO_3)_2{\cdot}3H_2O$ (5 mmol, Acros Organics, 99 %) and $ZrO(NO_3)_2{\cdot}6H_2O$ (5 mmol, Acros Organics, 99.5 %) were dissolved as separate solutions in deionised water (100 mL). The solutions were subsequently mixed together and stirred for 5 min. The temperature of the mixture was maintained at 25 °C with a heated water bath throughout this synthesis. The solution was subsequently adjusted to pH 4.5 by a slow and controlled addition of aqueous K_2CO_3 (0.2 M, Fisher Scientific, 99%). Once at pH 4.5, the mixture was aged for 30 min. After 30 min, the pH was adjusted to 5.5 and the mixture was left to age for another 30 min. The process was repeated for pH set points of 6.5, 7.5, and 9.5. Once a pH 9.5 was reached, the mixture was aged for 4 h. Once the ageing process was complete, the catalyst was recovered by vacuum filtration and washed with deionised water (2 L, room temperature). The catalyst precursor was subsequently dried at 110 °C for 16 h. After drying, the catalyst was ground to a fine powder using mortar and pestle and calcined under static air at 400 °C, 20 °C min^{-1} for 4 h. A series of catalysts with different copper loadings (10–50 mol%) were prepared this way. Some of these catalysts were subsequently subjected to an additional reductive heat treatment, in such cases, this was conducted under flowing 5% H_2/Ar (200 mL min^{-1}) at a range of temperatures with a ramp rate of 10 °C min^{-1} for 2 h.

In some cases, the calcined catalysts were stirred in 0.5M HNO_3 for 20 min (100 mL $g^{-1}_{catalyst}$). The catalyst was then centrifuged and washed. The washing process was repeated until pH of the decanted solution was neutral (typically three washes). The catalyst was then dried at 110 °C for 16 h.

2.2. Catalyst characterisation

Powder X-ray diffraction (XRD) was performed on a PANalytical X'Pert Pro diffractometer with a monochromatic Cu-*K*α source (λ = 0.154 nm) operated at 40 kV and 40 mA. The 2θ scan range was between 10° and 80°.

Surface areas were determined by multi-point N_2 adsorption at 77 K on a Micromeretics Gemini 2360 according to the Brauner-Emmet-Teller (BET) method. Prior to the analysis, samples were degassed at 120 °C for 2 h under N_2 flow.

TPR was carried out using a Thermo 1100 series TPDRO. Samples (0.1 g) were pre-treated at 110 °C (heating rate = 20 °C min^{-1}) under Ar for 1 h prior to reduction in order to clean the surface. Analysis was performed under 10% H_2/Ar (BOC 99.99%, 25 ml min^{-1}) 30–500 °C, 1 °C min^{-1}.

Scanning electron microscopy (SEM) was carried out using a Tescan MAIA3 Triglav FEG-SEM, with the beam operating at 15 kV. Samples were prepared for SEM by depositing them onto a carbon-supported, 300-mesh copper grid, and drying any excess solvent. The sample was then sputter coated with a 7 nm layer of gold, in order to reduce charging of the catalyst from the electron beam.

Leaching studies were carried out using Agilent 4100 Microwave Plasma Atomic Emission Spectrometer (MPAES). The instrument was calibrated with solutions of known copper concentration, and filtered post-reaction solution was compared against the calibration curve.

X-ray photoelectron spectroscopy (XPS) was performed using a Kratos Axis Ultra-DLD photoelectron spectrometer, using monochromatic Al *Kα* radiation, operating at 144 W power. High resolution and survey scans were performed at pass energies of 40 and 160 eV respectively. Spectra were calibrated to the C (1*s*) signal at 284.8 eV, and quantified using CasaXPS v2.3.17, using modified Wagner sensitivity factors supplied by the manufacturer.

2.3. Catalyst testing

Hydrogenation of LA to GVL was carried out using a 50 mL stainless steel Parr 5500 autoclave equipped with a Teflon liner. In a typical experiment, the reactor was charged with 50 mg of catalyst, 0.5 g LA (Sigma Aldrich, 98%), 9.5 g distilled water, and purged three times with 35 bar H_2 in order to remove any residual gas. The autoclave was then heated to 200 °C. Once heated, the reactor was pressurized with 27 barg H_2; this was considered to be time zero. Reaction time was 2 h. After the reaction, the autoclave was cooled on ice, and the gasses were vented once the internal temperature was below 10 °C. The mixture was then filtered and analysed using a Varian 450 GC equipped with a CP-Sil 5CB column (50 m, 0.32 mm, 5 μm) and an FID detector. Tetrahydrofuran (Fisher Chemical, 99.5%) was used as an internal standard. Catalyst reuse testing was carried out by running a reaction with large amount of catalyst (0.25 g) under standard conditions. The catalyst was then filtered, washed with deionised water (100 mL) and dried at 110 °C for 16 h. From the used catalyst, 50 mg was taken and a standard reaction was carried out. This process was repeated for consecutive uses.

For the majority of the reactions conducted in this study repeat experiments were conducted in order to establish error margins for the reaction data. In such cases, the data point corresponds to the mean value determined and the positive and negative error bars are representative of the standard deviation across the data set.

3. Results and discussion

3.1. Co-precipitation by a pH gradient methodology

A series of Cu-ZrO_2 catalysts containing various Cu : Zr molar ratios were synthesised by a pH gradient method. This novel method of catalyst preparation was developed on the basis that Zr and Cu nitrate ligands will exchange with CO_3^{2-} ligands at a different pH. Cu nitrate and zirconyl nitrates can be precipitated by K_2CO_3 at pH 4–5 and 3–4, respectively. Indeed, it has been established that Cu precipitation is not fully achieved until an alkaline pH (above 9) is reached [34]. As such, we reasoned that by slowly increasing or decreasing the pH of this mixture, we could gain control over the distribution of Cu and Zr in the resultant mixed metal oxide. For the purpose of this investigation, we wanted to maximise the quantity of Cu on, or very close to, the surface of the material and therefore, created a synthesis procedure which involved ramping the pH slowly and in a controlled manner, over time. A graphical representation of this procedure is highlighted in Fig. 1(a).

For the initial investigations, a series of Cu-ZrO_2 with Cu loadings of 10, 20, 30, 40 and 50 mol% synthesised, calcined and tested for the hydrogenation of LA to GVL. The results from these experiments are displayed in Fig. 1(b). Clearly, there is a non-linear relationship between the Cu content of the catalyst and the yield of GVL produced, with the highest GVL yields observed in the reactions conducted over the 30 and 40 mol% catalysts. Interestingly, the GVL yield increases significantly as the Cu in the catalyst increases from 10 to 30 mol%, but not in a proportional manner; when the Cu content in the catalyst is doubled from 10 to 20 mol% for example, the yield of GVL produced triples. To investigate why this might be, the series of catalysts were characterised by BET, XRD and XPS.

The total surface areas of the materials, also illustrated in Fig. 1(b), follow a similar trend to the catalytic activity exhibited by the catalysts. This is unsurprising, as previous studies have reported that there is relationship between the total surface area and catalytic activity of Cu-ZrO_2 catalysts in this reaction [32,33]. The relationship between the GVL yield and surface area is similar but not proportional, indicating that the catalytic performance of these materials is not directly dictated by their total surface areas. Each of the samples was subsequently investigated by XRD; the corresponding diffraction patterns are displayed in Fig. 2. The materials with lower copper content (10%–30% Cu) appear to be amorphous and no distinct reflections could be observed. With the 40 mol% Cu material however, three distinct reflections characteristic of Cu(II)O (ICDD = 01-089-2529) emerge at 2θ = 36 °, 39 ° and 49 °. This indicated crystallite growth, likely attributed to the increased concentration of copper in the solution during the precipitation [35]. With the 50 mol% Cu material, the crystallite growth appears to be more significant, as several additional reflections characteristic of Cu(II)O appeared. Perhaps more interestingly, a small reflection at $2\theta = 31°$ also appeared which is characteristic of tetragonal zirconia (t-ZrO_2, ICDD = 01-080-3783). This indicates that with higher Cu loadings, a

phase separation occurs which would inevitably affect the distribution of Cu throughout the lattice of the material.

These observations would appear to tie in with the activity data; whilst increasing Cu loadings of 10%–30% display a strong increase in activity, increasing the loading beyond this point does not improve the activity. At the highest loadings, the activity decreases. The formation of the copper oxide phases at these loadings implies that copper is being deposited on the surface, as opposed to being intimately mixed with the surface lattice. This could act to lower the activity, which would be consistent with previous observations that copper deposited on the surface in large enough crystallites to be detected by XRD is inactive for this reaction. In addition to being less active, this surface copper could also act to lower the number of Cu-ZrO_x interface sites that we believe to be the active site for the reaction. This would have further detrimental effects on the activity.

The XRD patterns also demonstrate that Cu can be present in quite large quantities (up to 30 %) without the formation of detectable Cu or Cu(II)O structures. Presumably, this Cu is integrated into the zirconia lattice while at higher Cu loadings the lattice becomes saturated and Cu deposits on the material surface as a discrete phase.

Subsequent investigation of these materials by XPS provided information on the materials' surface elemental composition. The Cu (2*p*) and Zr (3*d*) regions for the catalytic series are presented in Fig. 3. The quantity of Cu on the surface steadily increased with rising Cu loading on the catalyst, whereas the quantity of Zr on the surface decreased marginally between 10%–40% Cu, and showed a large decrease in the 50% Cu catalyst. This could be due to the formation of large particles of copper oxide on the surface of the material; as XPS is a quasi-surface technique, copper oxide particles of sufficient size could act to occlude the underlying zirconia.

From calculation of the Cu/Cu+Zr ratio on the surface (Table 1) it was determined the surface Cu content was generally proportional to the total Cu loading of the catalysts, with increased Cu loadings only observed for the 50% loading. This would be consistent with the idea that large amounts of copper oxide have been deposited on the surface in the 50% Cu catalyst. However, the lack of surface copper enrichment means that the primary motivation for the development of the pH gradient method; to increase the proportion of Cu on the surface, had not been achieved. Nevertheless, the observation that the yield of GVL formed in the reaction is not proportional to the quantity of Cu on the surface may be informative for the identification of the active surface species in this reaction.

Subsequent experiments were conducted over the 30 mol% Cu-ZrO_2 catalyst in order investigate the stability of the catalyst as previously Cu-ZrO_2 catalysts prepared by co-precipitation have been reported to deactivate rapidly over subsequent uses [33,32]. GVL yield as a function of time in a typical experiment is shown in Fig. 4(a). The yield after 4 h reaction time is around 75% and in fact 100% yield is not observed after longer run times. As the only observed product is GVL this indicates

incomplete conversion of the LA substrate. This does indicate deactivation of the catalyst during a batch reaction, however, only trace quantities of Cu were detected by MP-AES after a standard conditions reaction; so that less than 0.2% of the Cu leached from the catalyst during a 2 h reaction. Even so, additional cycling experiments (Fig. 4b) confirmed that the catalytic performance of the 30 mol% catalyst remained reasonably constant for up to 4 uses, which is a marked improvement compared with other Cu-ZrO_2 catalysts we have investigated previously (activity drop of up to 30% after 1 use) [28,32]. Perhaps most interestingly, SEM confirmed that there was severe change in the surface morphology of the catalyst upon subsequent uses, see Fig. 5(a-d), which evidently has little effect on the catalysis taking place. This could be indicative of phase separation between Cu/CuO_x and ZrO_2, which is evidenced by evaluating the corresponding XRD patterns of each materials (Fig. 5e). The Cu crystallite sizes increase upon subsequent uses, which were estimated from the Cu(111) reflection using the Scherrer equation; at $2\theta = 43^{\circ}$. The observation that this substantial change in the morphology of these materials does not impact catalytic performance, indicates that the Cu/CuO_x particles on the surface of the catalyst are likely to be spectator species in this reaction and thus, are unlikely to be involved in the catalytic surface mechanism taking place. With this in mind we suggest that the deactivation observed over long run times (Fig. 4a) is likely due to site inhibition either by the GVL product or by an unidentified reaction intermediate which adheres to the active site. On reuse testing the catalyst is washed prior to reuse which could free up the active site for subsequent reaction runs.

3.2. Identification of the catalytically active species

We previously proposed that lattice Cu in close proximity to the surface of the catalyst is very important for the performance of Cu-ZrO_2 catalysts in this reaction [33]. To establish whether the large Cu/CuO_x particles on the surface were indeed spectator species, each of the catalysts was subjected to an acid treatment with HNO_3 (0.5 M) as described in the experimental section. The aim of these acid washing steps was to remove labile copper species and expose underlying copper species with SMSIs. To confirm that all the labile species had been removed, some of the acid-treated catalysts were subjected to a second acid wash, after which only negligible amounts of Cu were present in the resulting acidic solution. Analysis of the acid washings by MP-AES allowed for the determination of Cu metal leached from each of the catalysts. The results indicated that large amounts of Cu were removed from the catalysts; the quantity of Cu removed had a linear dependence on the original target Cu loading of each catalyst; only 1.3% was removed from the 10 mol% Cu-ZrO_2 catalyst, whereas 76.6% of the Cu present in the 50 mol% Cu-ZrO_2 was removed. As the quantity of Cu lost is not proportional to the quantity of Cu present in each catalyst, it indicates that during catalyst synthesis, copper species first saturate the bulk lattice before Cu is precipitated on to the surface.

Following the acid treatment, the catalysts were tested for hydrogenation of LA to GVL under standard conditions, the results of which are displayed in Fig. 6. Interestingly, it was determined that the catalysts retained their activity completely despite the loss of significant quantities of copper. Indeed, the 50% Cu catalyst was actually more active after having 76.6% of its copper removed. This strongly implies that the copper removed by acid washing is a spectator species that plays little part in the reaction. As the removed copper was not involved in the reaction, we can attribute the catalysis taking place to surface lattice Cu species with SMSIs. The resilience of the active species towards acid treatment underlines the stability of the catalyst. We also noted that there is negligible leaching of the zirconia support during the acid washing procedure

To further rationalise this data, the turnover frequency (TOF) of each catalyst was calculated and normalised to the moles of copper remaining on the acid-washed catalyst (Fig. 7). The quantity of Cu remaining in each of the catalysts was estimated by quantifying the amount of Cu leached during the acid treatment by MP-AES (Table 2). A linear trend was observed between the GVL yield observed and the copper content present in the catalysts. The acid-washed materials had higher TOFs than their fresh counterparts, further evidencing that much of the surface Cu species in the fresh catalysts are indeed spectator species. SEM images of the acid washed catalysts were subsequently obtained (Fig. 8a-d). The morphology of the catalysts was radically different to the fresh samples; there was no evidence to suggest that any large Cu/CuO_x particles were still present. With the 40 mol% and 50 mol% $Cu\text{-}ZrO_2$ catalysts, large pores were observed, evidencing the significantly large quantities of spectator Cu in the fresh catalysts. Despite this, the activity of the 50 mol% $Cu\text{-}ZrO_2$ did not decrease, and but understandably, the TOF improved drastically from 12.85 $mol_{GVL}\ mol_{Cu}^{-1}\ h^{-1}$ to 68.64 $mol_{GVL}\ mol_{Cu}^{-1}\ h^{-1}$.

3.3. Pre-reduction effects on catalytic performance

It is known that the reduction of copper is a highly exothermic process and that poor control of reduction conditions can lead to substantial sintering of heterogeneous catalysts [36]. Given that we have already established that the catalytic activity of the $Cu\text{-}ZrO_2$ catalyst is strongly related to intimate mixing of Cu and ZrO_2, we wanted to establish whether it was beneficial to pre-reduce the $Cu\text{-}ZrO_2$, prior to catalytic testing experiment. To investigate whether this pre-reduction was influential, our most active catalyst; the 30 mol% $Cu\text{-}ZrO_2$, was pre-reduced at various temperatures from 150 – 500 °C with 5% H_2/Ar. A slow temperature ramp (1 °C / min) was invoked to prevent, or at least reduce, any localised exotherms in the catalyst bed. H_2 TPR was used to establish the lowest reduction temperature which should be used (Fig. 9a).

XRD of the pre-reduced catalysts confirmed that the reduction temperature significantly influenced the crystallinity of the catalysts (Fig. 9b). Reflections at 2θ = 43°, 51° and 74°, which are characteristic of

metallic copper (ICDD = 01-070-3038) become more prominent as the reduction temperature increases. Assessment of the Cu (111) peak (2θ = 43°) by the Scherrer equation provided an estimation of the corresponding Cu crystallite sizes for each catalyst. As the reduction temperature was increased, the crystallinity of the Cu phase increased significantly (Table 3) and the particle sizes of the Cu species increased. This aligns with the surface area of the catalysts (Table 3), which decreases as the reduction temperature increases. After reduction at 500 °C, additional reflections at 2θ = 31°, 35°, 60° and 63° are observed, which are characteristic of tetragonal zirconia (t-ZrO_2, ICDD = 01-080-3783). Given that no characteristic reflections of ZrO_2 are present in in the XRD patterns for any of the other samples, it suggests that reduction at 500 °C leads to a complete phase separation between Cu and ZrO_2. Indeed, this was confirmed to be the case by subsequent investigation of the 30 mol% Cu-ZrO_2 catalysts reduced at 150 and 500 °C by SEM-EDS (Fig. 10b and c, respectively). Each of these catalysts was subsequently tested for the hydrogenation of LA (Fig. 10a). The reduction temperature had a profound effect on catalytic performance; activity decreased as reduction temperature increased. This aligns well with conclusions drawn previously, that an intimate mixing of Cu and Zr promotes catalytic performance in this reaction. Agglomeration of Cu or indeed ZrO_2, will likely result in a loss in catalytic performance. This is shown in the trend of increasing Cu particle size leading to less active catalysts.

4. Conclusions and future perspectives

A range of $CuZrO_2$ catalysts with varied molar copper content were synthesised by a novel pH gradient co-precipitation method. Their activity for the hydrogenation of LA was determined to be related to the total surface area of the catalysts. Further investigation confirmed that activity was in fact dictated by the degree of mixing between Cu and ZrO_2 phases; activity is considered to be directly related to the proportion of Cu/ZrO_x interface sites in a given catalyst. In typical co-precipitated catalysts, much of the copper in the final catalyst is but a spectator in the reaction. We have previously observed the important role lattice copper has on the performance of these catalysts but until now were unable to ascertain why. The new insights herein infer an intimately mixed copper-zirconia surface phase leads to highly active catalysts, which is in line with our assumption that the active site for this reaction is the interface between copper and zirconia upon reduction. This intimate mixing may also play a role in the increased stability of these catalysts relative to other examples in the literature. We consider that this enhanced understanding will be exceptionally important for future work in this abundant and heavily competitive area of research. Developing novel routes to synthesise Cu-ZrO_2 catalysts with SMSIs should be priority moving forward, to ensure that the process is as economic and atom efficient as possible.

Acknowledgments

This work was financially supported by the European Union FP7 NMP project NOVACAM (Novel cheap and abundant EU-Japan-604319).

Schemes and Figures

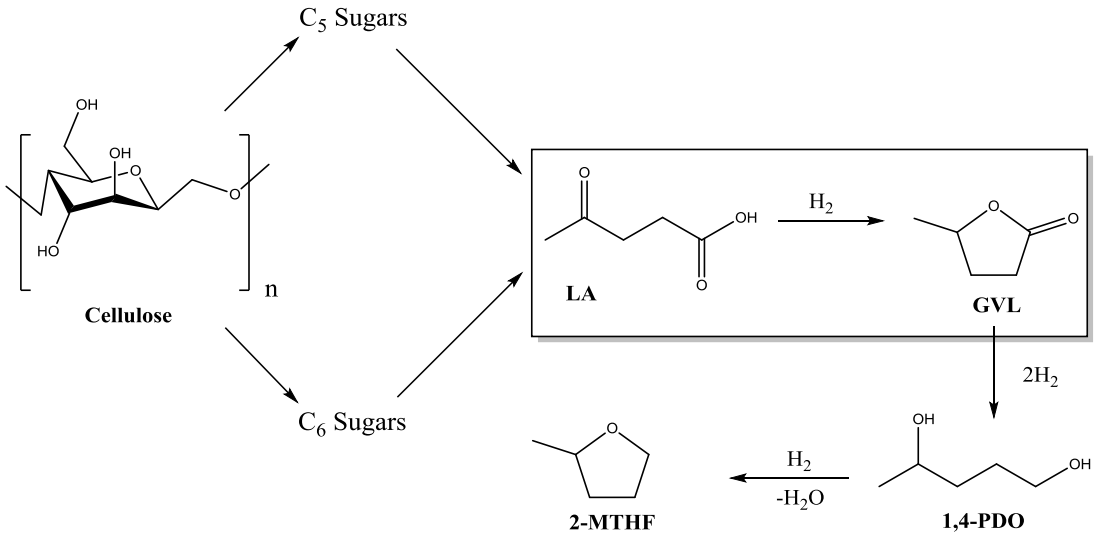

Scheme 1: Levulinic acid (LA) is formed from the hydrolysis of cellulose and can be hydrogenated to γ-valerolactone (GVL) over a suitable catalyst. GVL can also undergo sequential hydrogenation to 1,2-pentanediol (1,4-PDO) and 2-methyltetrahydrofurfural (2-MTHF).

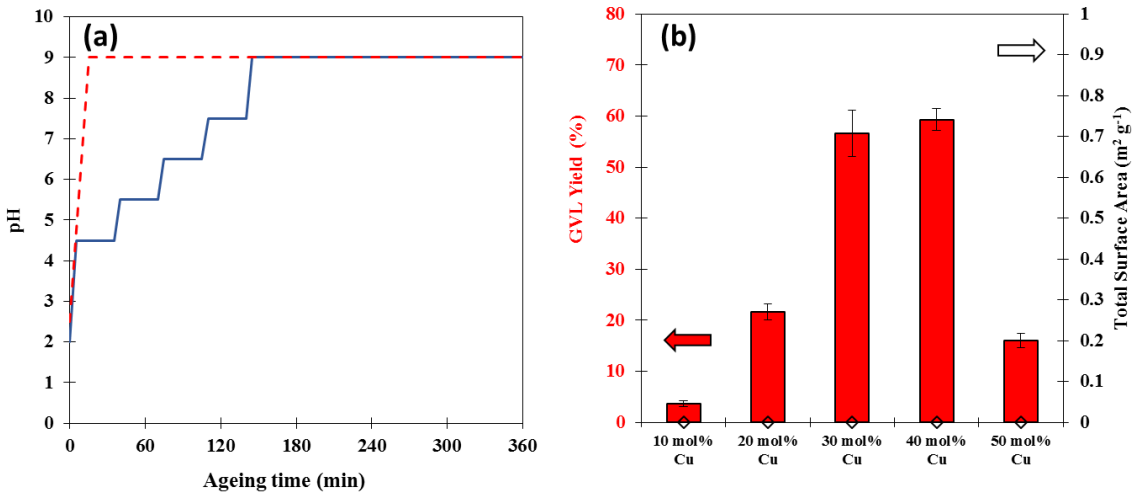

Fig. 1. A series of Cu-ZrO_2 catalyst with varied Cu/Zr loadings were prepared via a pH gradient methology (a); the dotted and solid lines correspond to the pH ramp in the standard and pH gradient methods, respectively. The activity of the catalysts for the hydrogenation of LA to GVL and their total surface area as determined by BET is displayed in (b). Reaction conditions: 200 °C; H_2 27 bar; 2 h; substrate 5 wt% LA/H_2O (10 g); catalyst (0.05 g).

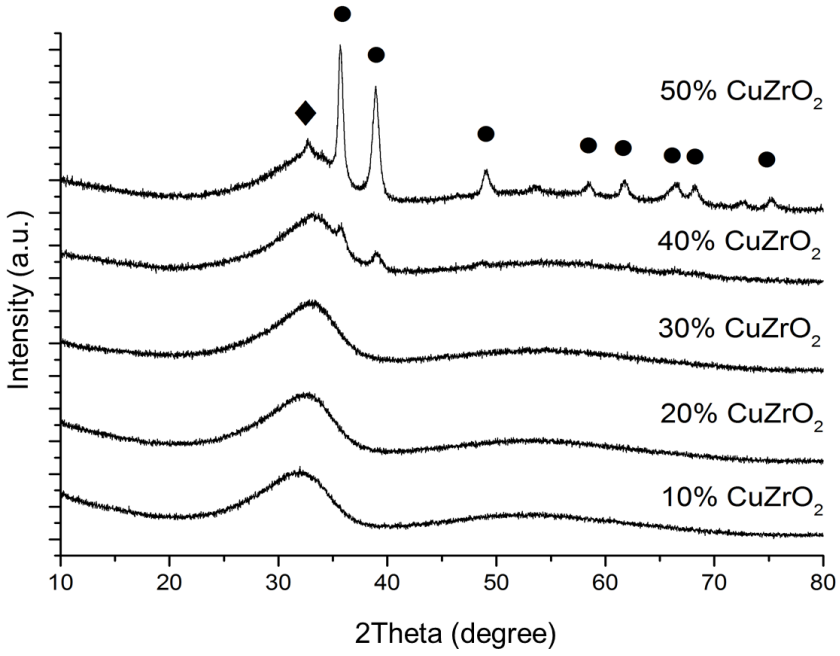

Fig. 2: XRD diffraction patterns corresponding to the series of Cu-ZrO_2 catalysts prepared by the pH gradient methodology. ● CuO; ♦ t-ZrO_2.

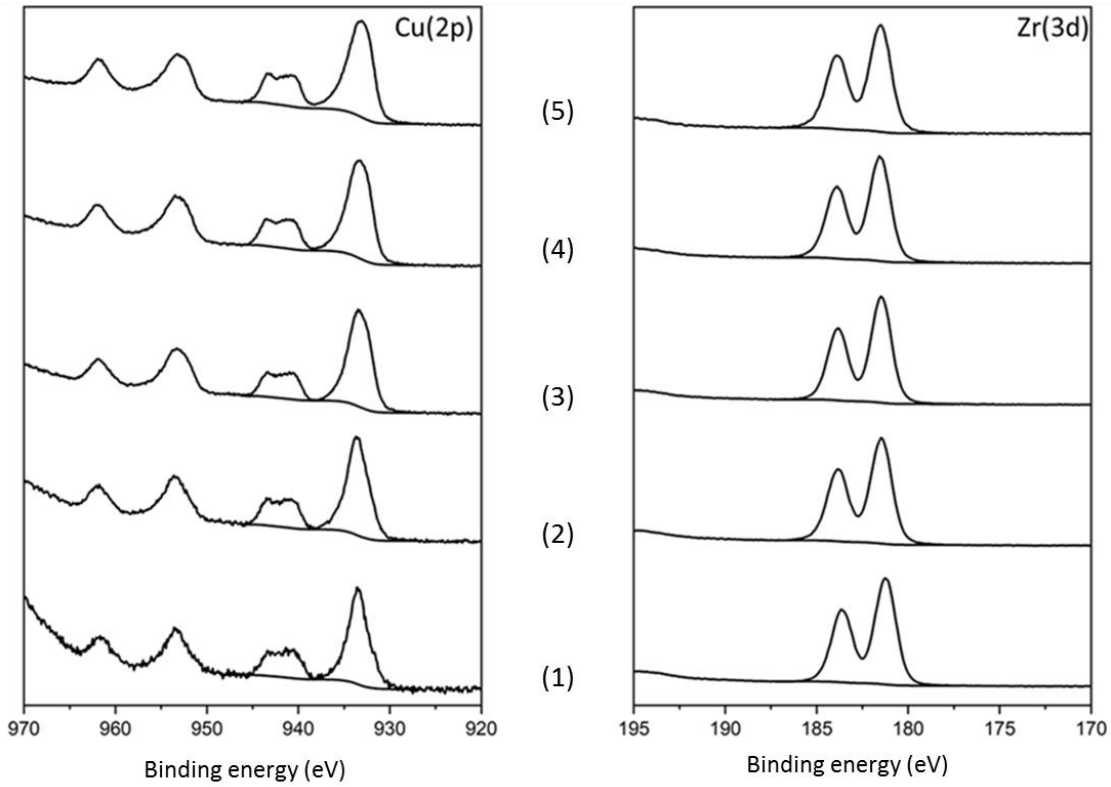

Fig. 3: X-ray photoelectron spectra of the Cu(2*p*) and Zr(3*d*) regions for (1) 10 mol% Cu-ZrO_2, (2) 20 mol% Cu-ZrO_2, (3) 30 mol% Cu-ZrO_2, (4) 40 mol% Cu-ZrO_2 and (5) 50 mol% Cu-ZrO_2 catalysts.

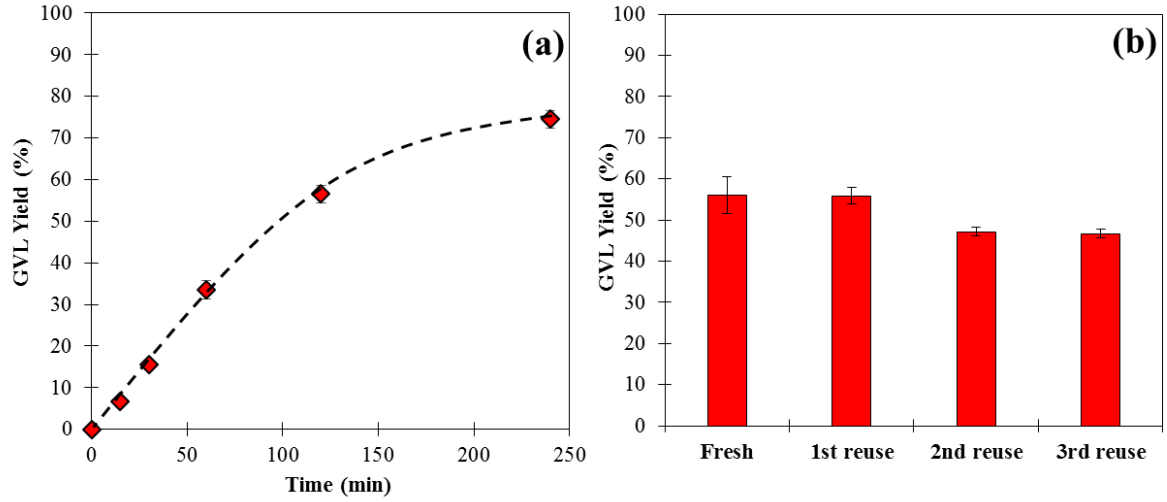

Fig. 4. (a) The yield of GVL produced as a function of time for the hydrogenation of LA over a 30 mol% Cu-ZrO_2 catalyst. (b) Investigation into how the activity of the 30 mol% catalyst is effected by sequential reactions; 2 h reactions. Reaction conditions: 200 °C, H_2 27 bar, time stated, substrate 5 wt% LA/H_2O (10 g), catalyst (0.05 g).

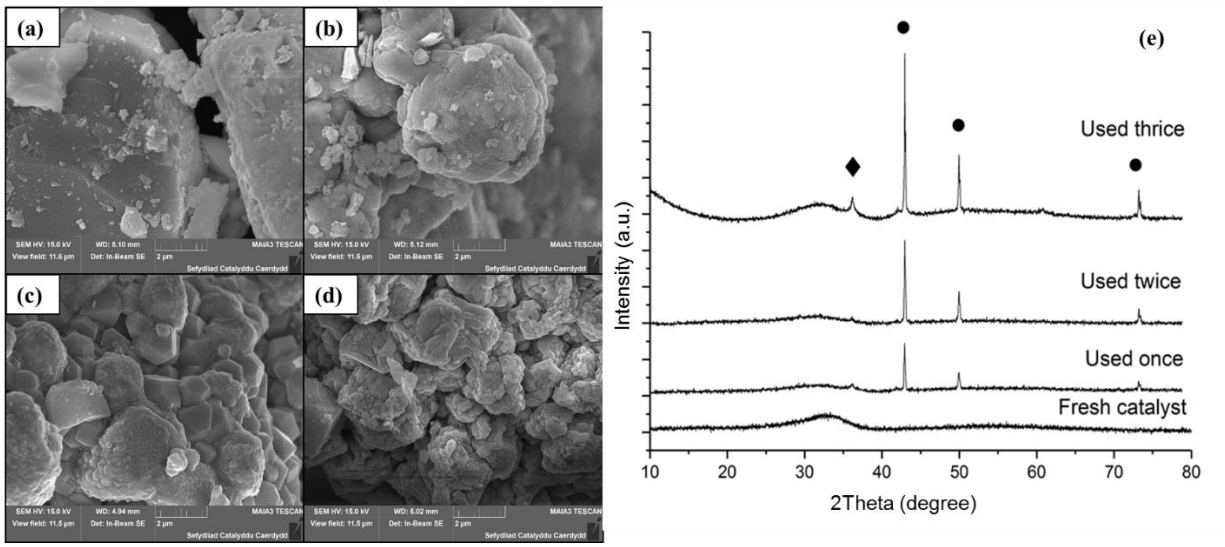

Fig. 5. Characterisation of the fresh 30 mol% Cu-ZrO_2 catalyst (a), after one use (b), after two uses (c) and after three uses (d) by SEM. The XRD patterns for each of these samples are also displayed (e). For the XRD data series: ● Cu; ♦ t-ZrO_2. Cu crystallite sizes of 63, 74 and 87 nm were determined for the catalysts after one, two and three uses, respectively. The Cu crystallite sizes were estimated using the Scherrer equation (2θ = 43º).

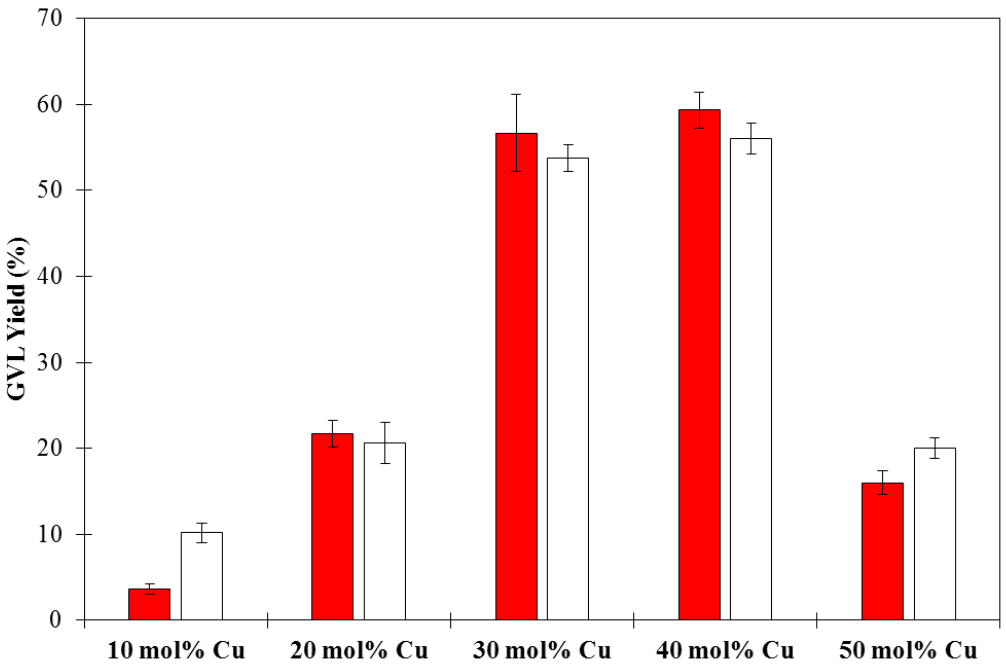

Fig. 6. The activity of the catalytic series before ■ and after □ treatment with HNO_3 (0.5 M). Reaction conditions: 200 °C; H_2 27 bar; 2 h; substrate 5 wt% LA/H_2O (10 g); catalyst (0.05 g).

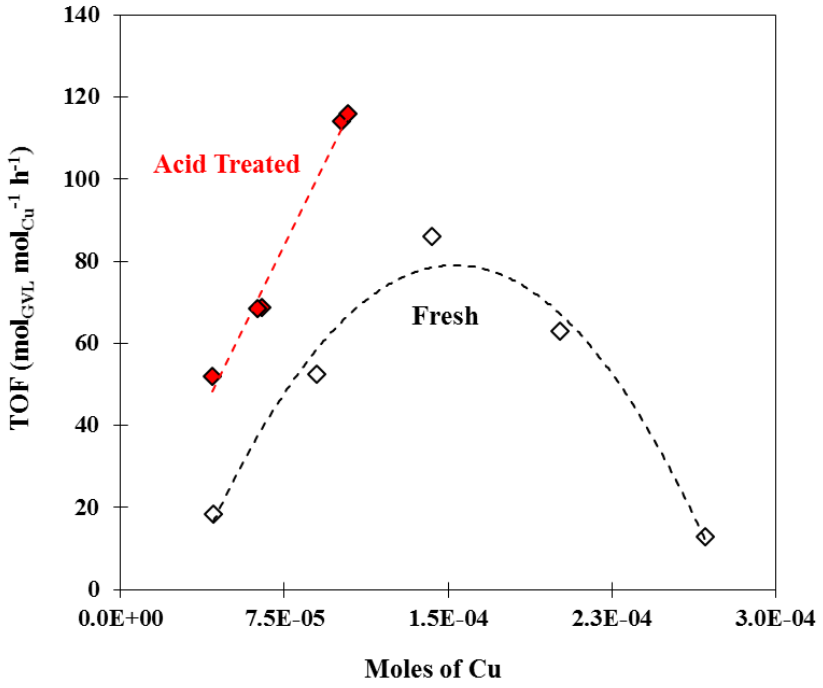

Fig. 7. Catalyst TOF dependence on moles of Cu present in the reactor. Comparison between the fresh; ◆ and acid washed; ◆ catalysts.

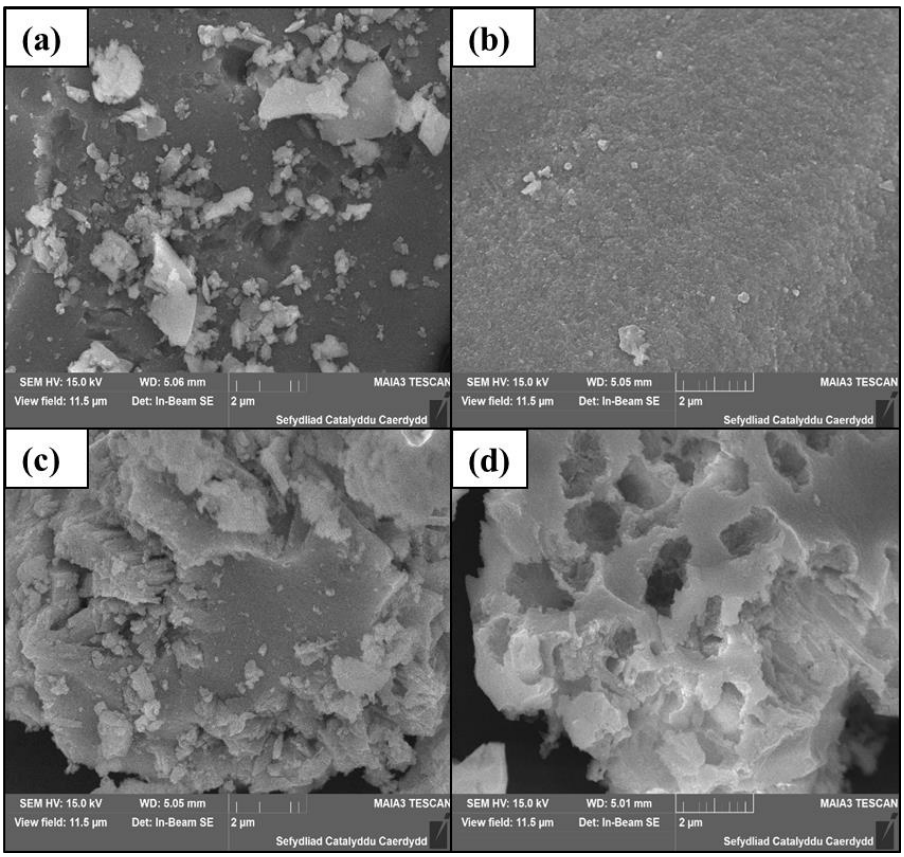

Fig. 8. SEM images of (a); the fresh (calcined) 10 mol% $CuZrO_2$ catalyst (b); 10 mol% $CuZrO_2$ after acid washing with HNO_3 (0.5 M) (c); fresh (calcined) 50% $CuZrO_2$ catalyst and (d); 50% $CuZrO_2$ after acid washing with HNO_3 (0.5 M).

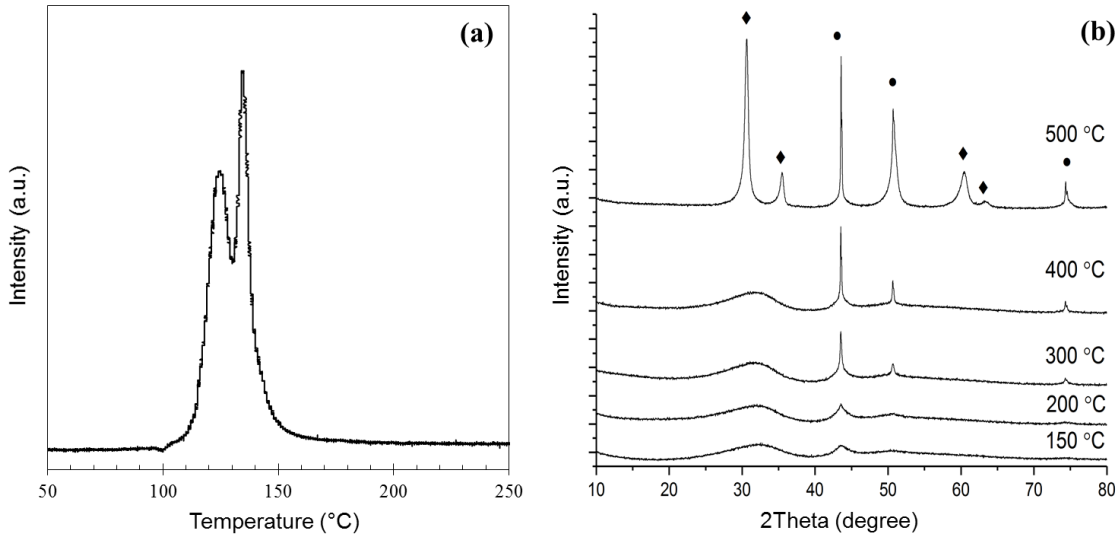

Fig. 9. Temperature programmed reduction of the calcined 30 mol% Cu-ZrO_2 catalyst with 5% H_2/Ar at a ramp rate of 1 °C/min (a). X-ray diffraction patterns of the calcined 30 mol% Cu-ZrO_2 catalyst after reduction at different temperatures (b).

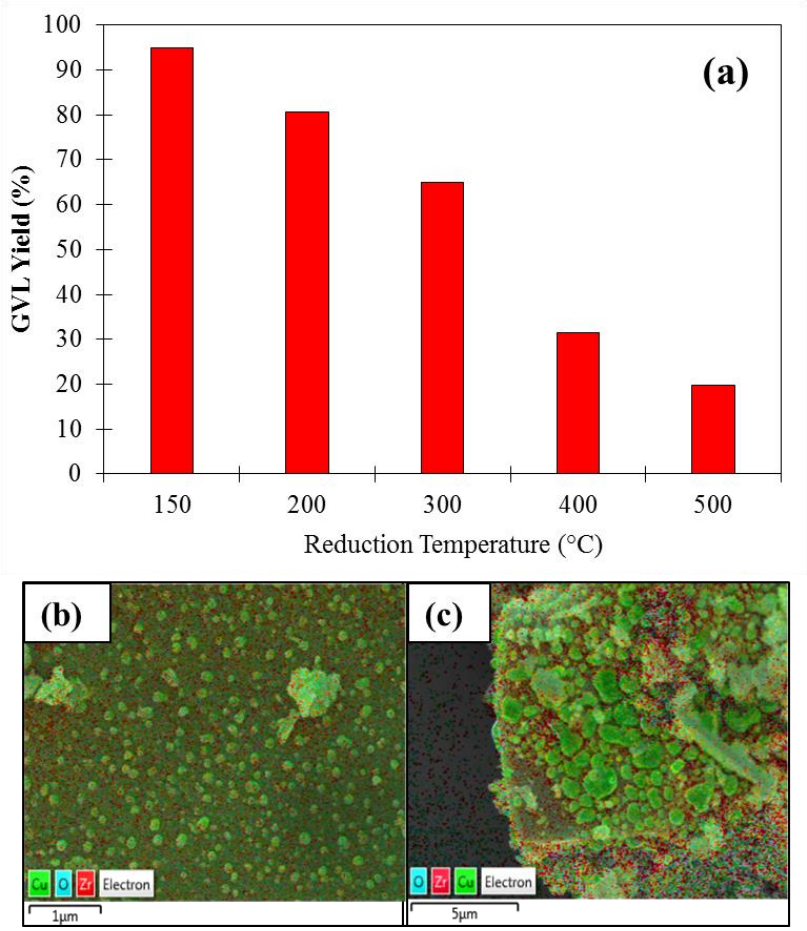

Fig. 10. Catalytic testing data for the calcined 30 mol% Cu-ZrO_2 catalyst after reduction at different temperatures (a). SEM images of the calcined 30 mol% Cu-ZrO_2 catalyst after reduction at 150 °C (b) and 500 °C (c).

Tables

Table 1. Surface atom coverage derived from XPS of the calcined calcined catalysts prepared by the pH gradient method.

Catalyst	Surface elemental concentrations (Atom %)				Atomic ratio (Cu/Zr)
	Cu (2*p*)	O (1*s*)	C (1*s*)	Zr (3*d*)	
10 mol% Cu-ZrO_2	2.32	50.57	24.15	22.97	0.09
20 mol% Cu-ZrO_2	5.47	53.02	18.27	23.24	0.19
30 mol% Cu-ZrO_2	9.21	54.58	14.17	22.04	0.29
40 mol% Cu-ZrO_2	12.93	54.88	11.8	20.39	0.39
50 mol% Cu-ZrO_2	19.74	51.65	12.69	15.91	0.55

Table 2. Quantified amounts of copper and zirconia lost upon acid washing the catalysts. MP-AES was used to quantify the effluent after washing with HNO_3 (0.5 M).

Catalyst	Copper lost (%)	Copper loading post acid treatment (mol%)	Zirconia lost (%)
10% Cu-ZrO_2	1.3	9.9	0.2
20% Cu-ZrO_2	28.2	14.4	0.4
30% Cu-ZrO_2	28.9	21.3	0.3
40% Cu-ZrO_2	48.4	20.6	0.6
50% Cu-ZrO_2	76.6	11.7	0.4

Table 3. BET surface area and Cu-crystallite sizes of the 30 mol% Cu-ZrO_2 catalyst after reduction at different temperatures.

Reduction temperature[a] (°C)	BET surface area ($m^2\ g^{-1}$)	Cu crystallite size[b] (nm)
150	-	-
200	50	6
300	28	25
400	9	75
500	11	87

[a]Catalysts reduced in 5 % H_2/Ar at stated temperature for 2 h. A ramp rate of 1 °C min^{-1} was used for each catalyst.
[b]Cu crystallite sizes were derived from XRD patterns of the corresponding catalysts using the Scherrer equation ($2\theta = 43^o$).

References

[1] W. Schutyser, T. Renders, S Van den Bosch, S.F. Koelewijn, G.T. Beckham, B.F. Sels, Chem. Soc. Rev. 47(2018)852-908.

[2] R.A. Sheldon, Green Chem. 16(2014)950-963.

[3] J.J. Bozell, G.R. Petersen, Green Chem. 12(2010)539-554.

[4] P. Lenihan, A. Orozco, E. O'Neill, M.N.N. Ahmad, D.W. Rooney, G.M. Walker, Chem. Eng. J. 156(2010)395-403.

[5] J.F.L. Silva, R. Grekin, A.P. Mariano, R. Maciel, Energy Technol. 6(2018)613-639.

[6] Q. Xu, X.L. Li, T. Pan, C.G. Yu, J. Deng, Q.X. Guo, Y. Fu, Green Chem. 18(2016)1287-1294.

[7] X.L. Du, Q.Y. Bi, Y.M. Liu, Y. Cao, H.Y. He, K.N. Fan, Green Chem. 14(2012)935-939.

[8] J.A. Melero, J. Iglesias, A. Garcia, Energy Environ. Sci. 5(2012)7393-7420.

[9] L.E. Manzer, Appl. Catal., A 272(2004)249-256.

[10] I.T. Horvath, H. Mehdi, V. Fabos, L. Boda, L.T. Mika, Green Chem. 10(2008)238-242.

[11] D.M. Alonso, S.G. Wettstein, J. A. Dumesic, Green Chem. 15(2013)584-595.

[12] J.Q. Bond, D.M. Alonso, D. Wang, R.M. West, J.A. Dumesic, Science 327(2010)1110-1114.

[13] R. Rathmann, A. Szklo, R. Schaeffer, Renew. Energy 35(2010)14-22.

[14] M.M. Gui, K.T. Lee, S. Bhatia, Energy 33(2008)1646-1653.

[15] M.B. Sainz, In Vitro Cell. Dev. Biol. Plant 45(2009)314-329.

[16] J.J. Tan, J.L. Cui, T.S. Deng, X.J. Cui, G.Q. Ding, Y.L. Zhu, Y.W. Li, Chemcatchem 7(2015)508-512.

[17] Z.P. Yan, L. Lin, S.J. Liu, Energy Fuels 23(2009)3853-3858.

[18] S. Cao, J.R. Monnier, C.T. Williams, W.J. Diao, J.R. Regalbuto, J. Catal. 326(2015)69-81.

[19] K. Yan, T. Lafleur, G.S. Wu, J.Y. Liao, C. Ceng, X.M. Xie, Appl. Catal., A 468(2013)52-58.

[20] K.Yan, T. Lafleur, C. Jarvis, G.S. Wu, J. Clean. Prod. 72(2014)230-232.

[21] K.Mustafin, F. Cardenas-Lizana, M.A. Keane, J. Chem. Technol. Biotechnol. 92(2017)2221-2228.

[22] P.P. Upare, J.M. Lee, D.W. Hwang, S.B. Halligudi, Y.K. Hwang, J.S. Chang, J. Ind. Eng. Chem. 17(2011)287-292.

[23] A.M. Hengne, C.V. Rode, Green Chem. 14(2012)1064-1072.

[24] L. Zhang, J.B. Mao, S.M. Li, J.M. Yin, X.D. Sun, X.W. Guo, C.S. Song, J.X. Zhou, Appl. Catal., B 232(2018),1-10.

[25] S. Pendem, I. Mondal, A. Shrotri, B.S. Rao, N. Lingaiah, J. Mondal, J. Sustain. Energy. Fuels 2(2018)1516-1529.

[26] D.R. Jones, S. Iqbal, L. Thomas, S. Ishikawa, C. Reece, P.J. Miedziak, D.J. Morgan, J.K. Bartley, D.J. Willock, W. Ueda, G.J. Hutchings, J. Catal. Struct. React. 4(2018)12-23.

[27] S.C. Patankar, G.D. Yadav, ACS Sustain. Chem. Eng. 3(2015)2619-2630.

[28] J. Hirayama, I. Orlowski, S. Iqbal, M. Douthwaite, S. Ishikawa, P.J. Miedziak, J.K. Bartley, J. K. Edwards, Q. He, R.L. Jenkins, T. Murayama, C Reece, W. Ueda, D.J. Willock, G.J. Hutchings, J. Phys. Chem., C, (2018)(**DOI: 10.1021/acs.jpcc.8b07108**)

[29] W.B. Gong, C. Chen, R.Y. Fan, H.M. Zhang, G.Z. Wang, H.J. Zhao, Fuel 231(2018)165-171.

[30] M. Chia, J.A. Dumesic, Chem. Commun. 47(2011)12233-12235.

[31] A. Corma, M.E. Domine, S. Valencia, J. Catal. 215(2003)294-304.

[32] D.R. Jones, S. Iqbal, S. Ishikawa, C. Reece, L.M. Thomas, P.J. Miedziak, D.J. Morgan, J.K. Edwards, J.K. Bartley, D.J. Willock, G.J. Hutching, Catal. Sci. Technol. 6(2016)6022-6030.

[33] S. Ishikawa, D.R. Jones, S. Iqbal, C. Reece, D.J. Morgan, D.J. Willock, P.J. Miedziak, J.K. Bartley, J.K. Edwards, T. Murayama, W. Ueda, G.J. Hutchings, Green Chem. 19(2017)225-236.

[34] J.W. Patterson, R.E. Boice, D. Marani, Environ. Sci. Technol. 25(1991)1780-1787.

[35] N.T.K. Thanh, N. Maclean, S. Mahiddine, Chem. Rev. 114(2014)7610-7630.

[36] S.A. Kondrat, P.J. Smith, P.P. Wells, P.A. Chater, J.H. Carter, D.J. Morgan, E.M. Fiordaliso, J.B. Wagner, T.E. Davies, L. Lu, J.K. Bartley, S.H. Taylor, M.S. Spencer, C.J. Kiely, G.J. Kelly, C.W. Park, M.J. Rosseinsky, G.J. Hutchings, Nature 531(2016)83-87.

Graphical Abstract

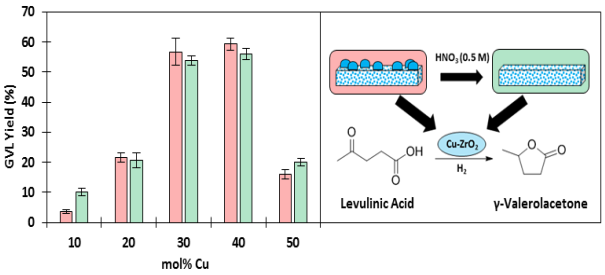

Description

Cu-ZrO_2 catalysts were synthesised by a pH gradient methodology, characterised and tested for the hydrogenation of levulinic acid to γ-valerolactone. The results from these experiments provide fresh insight on the intrinsic activity of these catalysts in hydrogenation reactions.